

# Size-Dependent Antibacterial Immunity of *Staphylococcus aureus* Protoplast-Derived Particulate Vaccines

This article was published in the following Dove Press journal:  
International Journal of Nanomedicine

Xuelian Fan<sup>1</sup>  
Fei Wang<sup>1</sup>  
Xin Zhou<sup>1</sup>  
Bin Chen<sup>2</sup>  
Gang Chen<sup>1</sup>

<sup>1</sup>Institute of Comparative Medicine, College of Veterinary Medicine, Jiangsu Co-Innovation Center for Prevention and Control of Important Animal Infectious Diseases and Zoonoses, Joint International Research Laboratory of Agriculture and Agri-Product Safety, The Ministry of Education of China, Yangzhou University, Yangzhou 225009, People's Republic of China; <sup>2</sup>Institute of Plant Resources and Chemistry, Nanjing Research Institute for Comprehensive Utilization of Wild Plants, Nanjing 210042, People's Republic of China

Correspondence: Gang Chen  
Institute of Comparative Medicine,  
College of Veterinary Medicine, Jiangsu  
Co-Innovation Center for Prevention and  
Control of Important Animal Infectious  
Diseases and Zoonoses, Joint  
International Research Laboratory of  
Agriculture and Agri-Product Safety, The  
Ministry of Education of China, Yangzhou  
University, 88 Daxue South Road,  
Yangzhou 225009, People's Republic of  
China  
Tel +86 0514-87931730  
Email gang\_chen2015@163.com

Bin Chen  
Institute of Plant Resources and  
Chemistry, Nanjing Research Institute for  
Comprehensive Utilization of Wild Plants,  
7 Jiangyun Road, Nanjing 210042, People's  
Republic of China  
Tel +86 025-85472025  
Email chen\_bin\_nj@163.com

**Background:** Vaccination provides a viable alternative to antibiotics for the treatment of drug-resistant bacterial infection. Bacterial protoplasts have gained much attention for a new generation vaccine due to depleting toxic outer wall components.

**Purpose:** The objective of this study was to reveal the effects of bacterial protoplast-derived nanovesicles (PDNVs) size on antibacterial immunity.

**Methods:** Herein, we prepared bacterial PDNVs with different sizes by removing the cell wall of *Staphylococcus aureus* (*S. aureus*) to generate multi-antigen nanovaccines. Furthermore, we investigated the ability of PDNVs in different sizes to activate dendritic cells (DCs) and trigger humoral and cellular immune responses in vivo.

**Results:** We obtained particles of ~200 nm, 400 nm, and 700 nm diameters and found that all the PDNVs readily induce efficient maturation of DCs in the draining lymph nodes of the vaccinated mice. Dramatically, the activation of DCs was increased with decreasing particle sizes. In addition, vaccination with PDNVs generated elevated expression levels of specific antibody and the production of INF- $\gamma$ , especially the smaller ones, indicating the capability of inducing strong humoral immunity and Th1 biased cell responses against the source bacteria.

**Conclusion:** These observed results provide evidence for size-dependent orchestration of immune responses of PDNVs and help to rationally design and develop effective antibacterial vaccines.

**Keywords:** nanoparticles, protoplasts, size, bacterial vaccines

## Introduction

*Staphylococcus aureus* (*S. aureus*), a typical human pathogenic bacterium, has become a significant threat to global public health with the incidence of associated infectious diseases increasing continually.<sup>1</sup> Overuse of antibiotic regimens leads to the emergence of resistance, which presents a great challenge to clinical treatment. Drug-resistant *S. aureus* can induce severe skin lesions, pneumonia, bacteremia and meningitis life-threatening diseases.<sup>2</sup> As highlighted by the World Health Organization (WHO) recent report, *S. aureus* spread worldwide, which is majorly responsible for high mortality by multidrug-resistant organism infection.<sup>3</sup> With the development of new antibiotics near stagnant, exploration in novel antibacterial strategies against drug-resistant *S. aureus* infections is crucial.<sup>4-6</sup> Vaccination has become a promising approach for preventing or treating infectious diseases, which is easy operation, extensive application, and possesses the ability of generating

long-term protection.<sup>3,7</sup> Training host immune systems to recognize and combat pathogens by vaccination can be leveraged to enhance the ability of innate immunity and induce highly specific responses against pathogens in adaptive immunity.<sup>1,8,9</sup>

Recently, bacterial derivatives, such as extracellular vesicles (EVs, also known as outer membrane vesicles [OMVs] in Gram-negative bacteria) and protoplast-derived nanovesicles (PDNVs) have emerged as attractive vaccines or delivery systems.<sup>10–12</sup> Both EVs and PDNVs contain various biological immune stimulating components with the ability of activation immune system.<sup>13</sup> They are spherical non-replicating vesicles formed with bilayered membrane, which incorporate with various bacterial proteins, polysaccharides, lipids and nucleic acids. Recent studies have shown that EVs with inherently multi-antigen and immunostimulatory is a reliable vaccine platform.<sup>14,15</sup> EV vaccines against *N. meningitidis* shown great clinical efficacy in Cuba, Norway, and New Zealand.<sup>16</sup> However, EVs usually contain some virulence factors, such as endotoxin lipopolysaccharide (LPS), pneumolysin (Ply), and pore-forming toxin Cytolysin A (ClyA) derived from bacteria.<sup>17</sup> Therefore, the safety of EVs limits their further application. In addition, the relatively low quantities of EVs released from bacteria will result in a high cost.<sup>18</sup> In contrast, PDNVs are harvested by removing the cell wall of bacteria where most of the bacterial toxins located. Due to the depletion of the toxic components on the cell wall, PDNVs are believed to be safe for use as vaccines or drug delivery vectors.<sup>19</sup> Also, as the development of nanotechnology, crude protoplasts are micro-sized vesicles which have a broad range of size adjustability providing attractive options for optimizing the vaccine delivery systems.<sup>20,21</sup>

Nowadays, increasing studies showed the size of particulate vaccines strongly influence vaccine properties.<sup>22,23</sup> Rational designs of vaccines on particular size will achieve orchestrating immune responses. Upon peripheral injection, the vaccines are taken up by antigen presenting cells (APCs) or directly enter the afferent lymphatic vessels and traffick to the secondary lymphoid tissue.<sup>24,25</sup> Sizes of particles will affect their routes of antigen delivery to the lymphoid tissue. Small sized particles (< 10 nm) can direct traffic into capillaries of circulatory system. Particles with the sizes of 10 ~ 200 nm can enter lymphatic capillary, while particles larger than 200 nm can be phagocytosed by partial APCs and migrated to lymph nodes.<sup>26,27</sup> Compared with transportation by APCs in

peripheral tissues, antigens targeting to lymph nodes directly can induce stronger immune responses due to abundant APCs, B cells, and T cells in lymphoid tissues.<sup>20</sup> Moreover, the APC activation and immune responses are also affected by particle sizes because of drainage and retention in lymph nodes. Smaller particles tend to be internalized more efficiently by APCs, while particles with larger size have better ability of retention in lymph nodes.<sup>28–30</sup> Despite a number of studies attempted to illustrate the corresponding rules between particle sizes and vaccination efficacies, most studies are focused on non-liposome particles.<sup>27,31</sup> Bacterial protoplasts have gained great attention as promising vaccine with lipid structures.<sup>32</sup> However, the effects of size on immune responses were still unknown.

In this study, in an attempt to optimizing vaccination efficacy, we prepared bacterial PDNVs with different sizes as multi-antigen vaccines (Figure 1). We then assessed the size, potential, morphology and stability of PDNVs. Furthermore, the size effects on APC activation, humoral and cellular immune responses were investigated in vivo.

## Materials and Methods

### Materials

BCA protein assay kit was purchased from the Beyotime Institute of Biotechnology (Haimen, China). FITC-conjugated anti-mouse CD11c antibody was purchased from BioLegend (San Diego, USA). PE-conjugated CD86 monoclonal antibody, PE-conjugated CD80 monoclonal antibody, and PE-conjugated CD40 monoclonal antibody were purchased from Invitrogen (Carlsbad, USA). Drug-resistant *S. aureus* BW15 was obtained from Dr. Gao (School of Medicine, Yangzhou University). Unless otherwise stated, all other reagents were purchased from the Nanjing Well Offer Biotechnology Co., Ltd. (Nanjing, China).

### Bacterial Culture and Preparation of PDNVs

Drug-resistant *S. aureus* BW15 were cultured on Luria broth (LB) agar overnight at 37 °C. Then a single colony was inoculated into LB medium. Following shaking at 250 rpm for 10–12 h, a 1:100 dilution of bacteria were further cultured until they reached late-logarithmic-phase. We first prepared EVs as positive control, the bacteria were centrifuged at 5000 g for 15 min. Then the medium were filtered through a 0.45 µm vacuum filter and the EVs

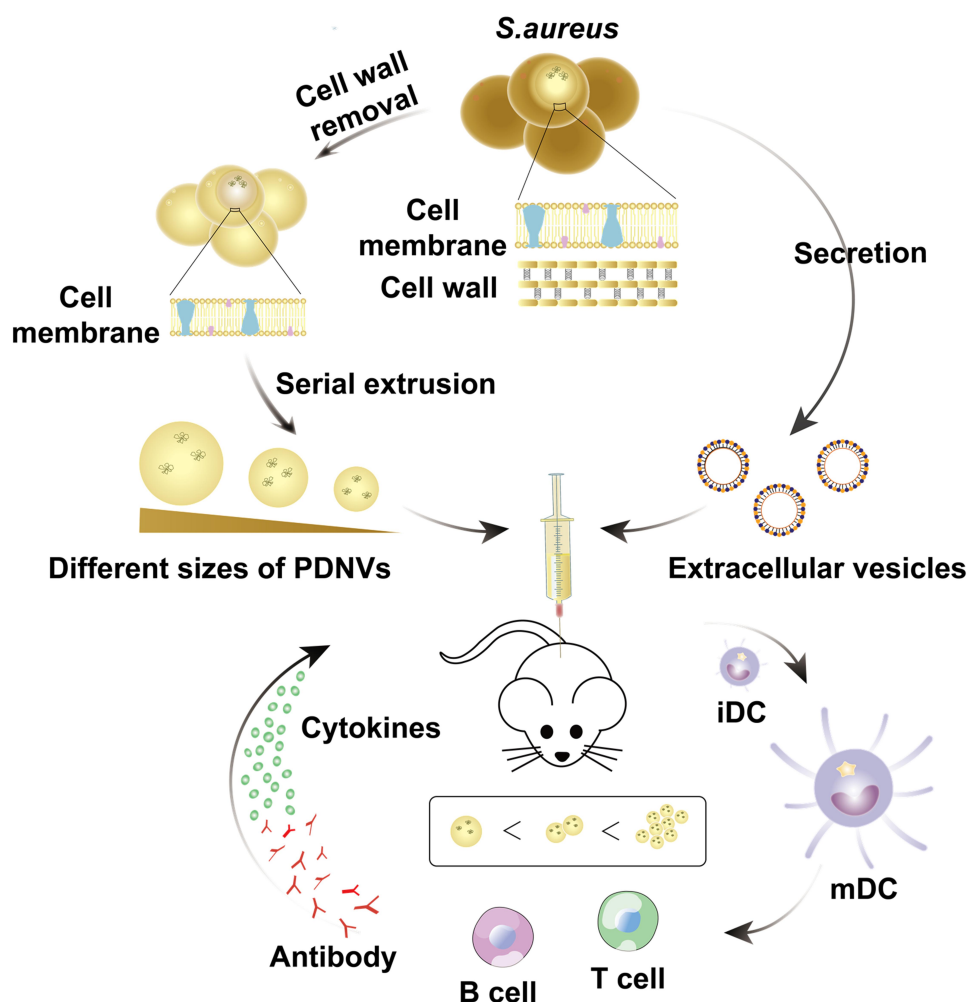


**Figure 1** A schematic illustration of size-dependent antibacterial immunity of *S. aureus* protoplast-derived particulate vaccines. Briefly, protoplasts were prepared by treating with lysozyme to remove the cell wall of *S. aureus*. Then the protoplasts were extruded serially through polycarbonate membranes to obtain different sizes of PDNVs. As a control group, EVs were prepared from the supernatant of bacterial cultures by ultracentrifugation. When injected subcutaneously into mice, PDNVs displayed size-dependent antibacterial immunity (iDC, immature DC; mDC, mature DC).

were pelleted by centrifuging at 150,000 g for 2 h at 4 °C (Beckman Coulter, California, USA).<sup>33</sup> To prepare PDNVs, EDTA was added slowly until the final concentration reached 10 mM and then incubated on a rotary shaker for 30 min. Then, the cells were centrifuged at 3000 g for 20 min and treated with lysozyme (2 mg/mL) at 37 °C for 1 h. The protoplast was harvested by centrifugation at 4000 g for 20 min at 4 °C.<sup>11</sup> Protoplast was then sequentially extruded thrice through 0.8, 0.4 and, 0.2 µm sized polycarbonate membrane filters with an Avanti mini-extruder to generate PDNV<sup>1</sup>, PDNV<sup>2</sup>, and PDNV<sup>3</sup>, respectively.

### Characterization of PDNVs

The hydrodynamic size, polydispersity (PDI) and zeta potential of a series of PDNVs were measured by Zeta

Plus (Malvern Instruments, Worcestershire, UK). The morphology of PDNVs with different sizes from *S. aureus* were investigated by transmission electron microscopy (TEM; Tecnai 12, Philips, Holland). The protein compositions of PDNVs were analyzed by SDS-PAGE. The stability of three different size PDNVs were evaluated by determining size changes incubated with PBS (pH 7.4) at different time points by Zeta Plus.

### Animal Care and Injections

The animal studies were approved by Jiangsu Province Administrative Committee for Laboratory Animals and complied with the guidelines of the Animal Care and Use Committee of Yangzhou University (Approval code: 201930788). Pathogen-free 5-week-old male C57BL/6 mice were purchased from Laboratory Animal Centre of

Yangzhou University, randomly grouped ( $n = 6$ ) and allowed to adapt the animal facility for one week before experiments. The mice were injected at the tail base via the subcutaneous routes with 5  $\mu\text{g}$  of PDNVs on day 0, day 7, and 14. EVs were used as the positive control and saline as the negative control.

## DC Maturation Induced by PDNVs with Different Sizes

For evaluating DC activation, inguinal lymph nodes were isolated 12 h after a single injection of PDNVs or EVs. The collected lymph nodes were teased with 26-gauge needles and digested into single cell suspensions by collagenase. Subsequently, cells were washed, blocked, and stained with fluorescently labelled anti-mouse antibodies against CD11c, CD86, CD80, and CD40. All the samples were analyzed by flow cytometry. A total of 10,000 cells were counted for analyze frequency.

## Bacterium-Specific Antibody Responses in vivo Induced by PDNVs with Different Sizes

One day before immunization, serum was collected and used to quantified antibacterial IgG antibodies by an ELISA assay. Ninety-six-well plate was coated with *S. aureus* and then blocked with 1% BSA. The blood serum was diluted by blocking buffer and 100  $\mu\text{L}$  diluted serum was loaded into the plate for incubating for 1 h at 37 °C. Then, the wells were treated with peroxidase-conjugated anti-mouse IgG for 1 h at 37 °C, then HRP-conjugated anti-mouse IgG antibody was added and incubated for 1 h at 37 °C. Finally, the antibacterial IgG antibodies were quantified by measuring the UV-Vis absorbance at 450 nm. The avidity detection was performed by incubating plates with urea (6 M) to remove the weak bound IgG before adding HRP-conjugated antibodies. The avidity index was defined as the ratio of IgG titer with urea to IgG titer without urea.

## Bacterium-Specific T Cell Activation Responses in vivo Induced by PDNVs with Different Sizes

Mice were sacrificed and their spleens were collected from each group on day 21. The single splenocytes were prepared similar with DCs as illustrated above. The cells were resuspended with PBS and seeded onto 12-well plates with a density of  $2 \times 10^5$  cells/well. *S. aureus* were inactivated

by formalin and  $1 \times 10^7$  CFU of bacteria were added to each well incubating for 3 days. After that, the concentrations of IFN- $\gamma$  and IL-4 in supernatants were quantified using ELISA assays.

## Statistical Analysis

Statistical assessments were conducted using a two-sided Student's *t*-test for two groups ( $P < 0.05$  was considered statistically significant).  $*P < 0.05$ ,  $**P < 0.01$ ,  $***P < 0.005$ , vs. control or the relevant group, as illustrated in the figure legends. The results are shown as the means  $\pm$  SD.

## Results and Discussion

### Preparation and Characterization of PDNVs from *S. aureus*

In this study, PDNVs and EVs from drug-resistant *S. aureus* strains BW15 were prepared by established protocols (Figure 1).<sup>34</sup> The obtained PDNVs sequentially extruded through 0.8  $\mu\text{m}$ , 0.4  $\mu\text{m}$ , and 0.2  $\mu\text{m}$  polycarbonate membrane filters were named PDNV<sup>1</sup>, PDNV<sup>2</sup>, and PDNV<sup>3</sup>, respectively. Zeta Plus analysis showed the diameters of PDNV<sup>1</sup>, PDNV<sup>2</sup>, PDNV<sup>3</sup>, and EV was  $712 \pm 20.96$  nm,  $396 \pm 11.45$  nm,  $220 \pm 10.21$  nm, and  $142 \pm 10.96$  nm with PDI of  $0.39 \pm 0.01$ ,  $0.21 \pm 0.01$ ,  $0.23 \pm 0.01$ , and  $0.26 \pm 0.01$ , respectively (Figure 2A). All the vesicles displayed similar zeta potentials approximately  $-15$  mV as shown in Figure 2B. To compare the stability of PDNVs with different sizes, we used PBS to simulate physiologic ionic conditions and to study the colloidal stability of PDNVs. Changes in the hydrodynamic size of the vesicles were monitored for 7 days in PBS (Figure 2C). The results showed that the size of PDNV<sup>1</sup> changed a lot within 1 week. The average maximum diameter of PDNV<sup>1</sup> over the 7 days is  $682 \pm 95.19$  nm, while the minimum diameter is  $418.83 \pm 92.86$  nm, and the change is more than 200 nm. In contrast, the PDNV<sup>2</sup>, PDNV<sup>3</sup>, and EV showed negligible hydrodynamic size change during the whole period of the study. The results indicate that PDNVs with smaller size were more stable. The protein bands of PDNVs with different sizes were similar, which indicated the protein compositions of PDNVs were not be impaired in the process of preparation. Even PDNV with smaller particle size could provide abundant protein antigens (Figure 2D). The morphologies of representative PDNVs and EVs were determined by TEM (Figure 3). All vesicles presented as spherical particles. And these results observed in TEM were consistent with the sizes analyzed by Zeta Plus (Figure 2A).



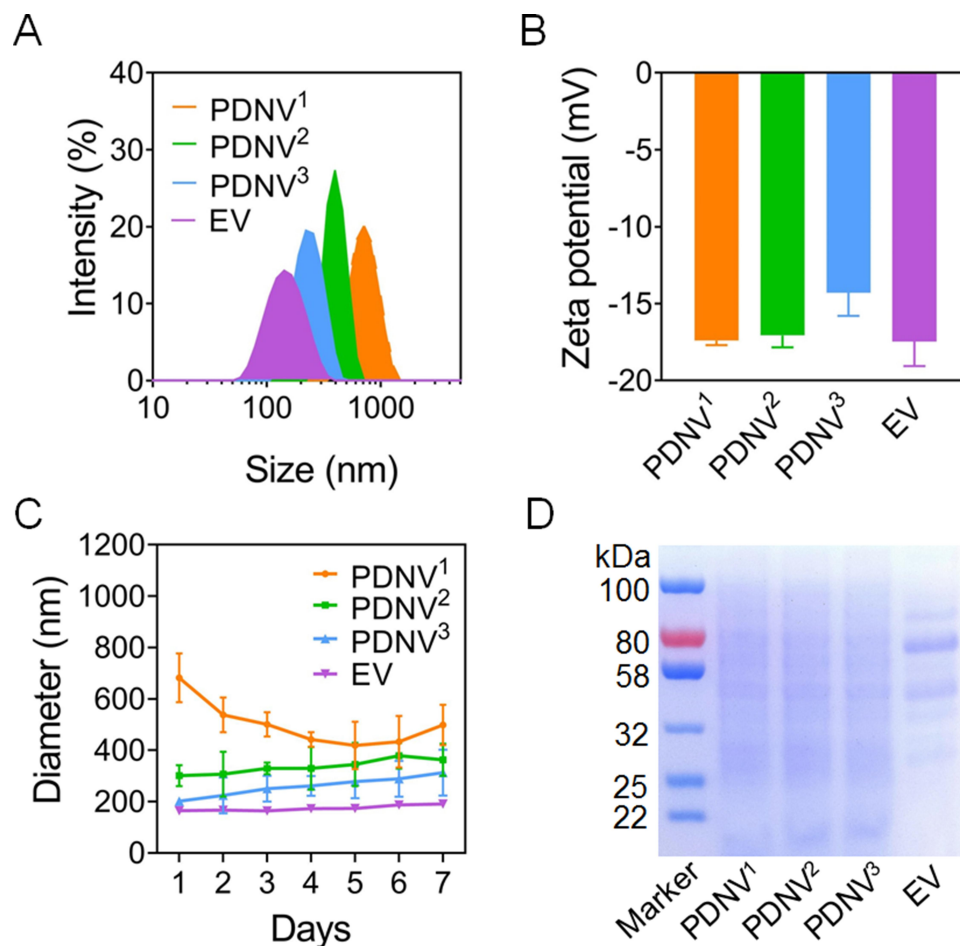


**Figure 2** Characterization of PDNVs with different sizes. **(A–B)** Hydrodynamic size (diameter, nm) and zeta potential of PDNVs. *S. aureus*-derived EVs were used as positive control. **(C)** Size changes of PDNVs in PBS buffer. **(D)** SDS-PAGE analysis of PDNVs. The molecular weights of a protein marker are shown on the left. Data are presented as means  $\pm$  SD ( $n = 3$ ).

## DC Maturation Induced by PDNVs with Different Sizes in vivo

We next evaluated the vaccine potential of PDNVs with different sizes in vivo. Mature DCs are the first line of cells in the initiation of antigen specific immune response, which were featured by upregulated expression levels of costimulatory molecules. Therefore, we analyzed the upregulation of CD86, CD80, and CD40 by DCs in the draining lymph nodes using flow cytometry.<sup>35–37</sup> Mice were divided into five groups ( $n = 6$ ) and injected subcutaneously at the tail base with PDNV<sup>1</sup>, PDNV<sup>2</sup>, PDNV<sup>3</sup>, EV (positive control), and PBS (negative control), respectively. Then the inguinal lymph nodes were collected after twelve hours of the injection. As shown in Figure 4A–C, compared with control group (CD86, 9.9%; CD80, 3.3%; CD40, 8.9%), all the PDNVs and EVs elevated the expression levels of CD86, CD80, and CD40 in DCs. PDNVs

with different sizes showed different expression levels of CD86 (PDNV<sup>1</sup>, 10.9%; PDNV<sup>2</sup>, 13.1%; PDNV<sup>3</sup>, 40.3%), CD80 (PDNV<sup>1</sup>, 7.3%; PDNV<sup>2</sup>, 13.9%; PDNV<sup>3</sup>, 35.3%), and CD40 (PDNV<sup>1</sup>, 19.3%; PDNV<sup>2</sup>, 24.6%; PDNV<sup>3</sup>, 41.6%). PDNV<sup>3</sup> displayed similar results with EVs (CD86, 43.5%; CD80, 31.8%; CD40, 45.6%) to promote DC maturation. These results indicated that smaller-sized PDNVs were able to induce more efficient activation of DCs by providing stronger co-stimulatory signals. These phenomena can be attributed to the superior stability of smaller particles as shown in Figure 2C. In addition, DC maturation requires efficient lymph node accumulation of antigens. Particles distribute to lymph nodes including active and passive ways and the fate depends strongly on particle size. Smaller particles ( $< 200$  nm) are hypothesized to be convected much easier through the interstitial flow, whereas larger particles require transport by tissue-

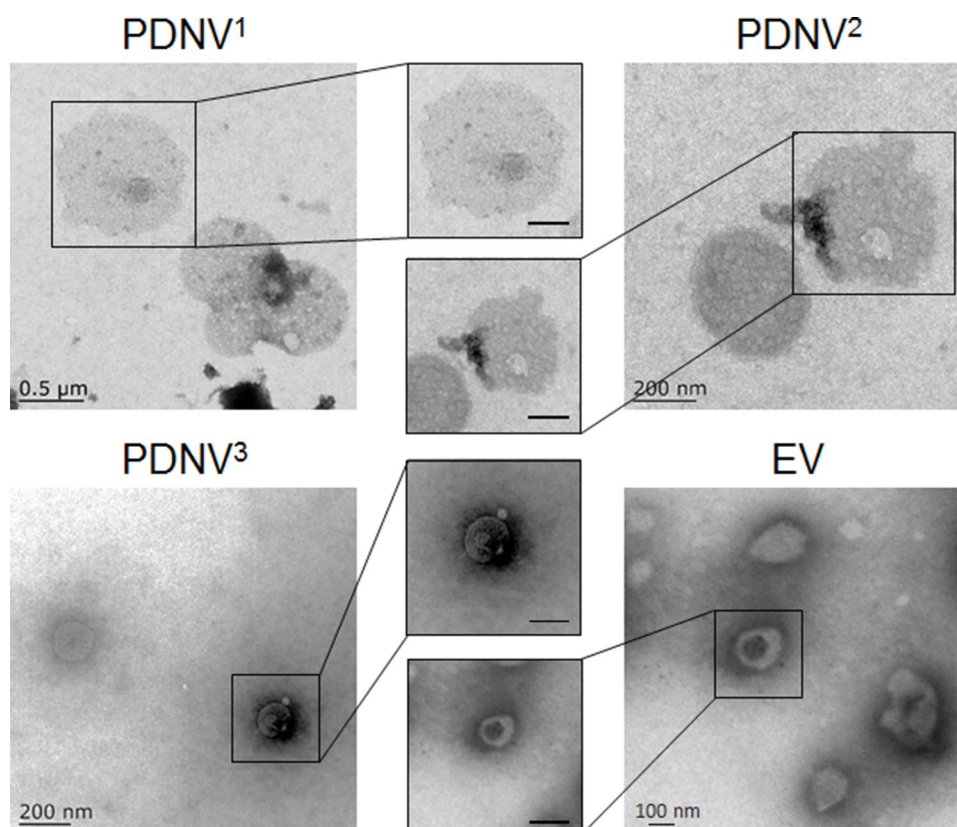


**Figure 3** Representative TEM images of PDNVs and EV from *S. aureus*. The scale bars of the inserted panels are 200 nm.

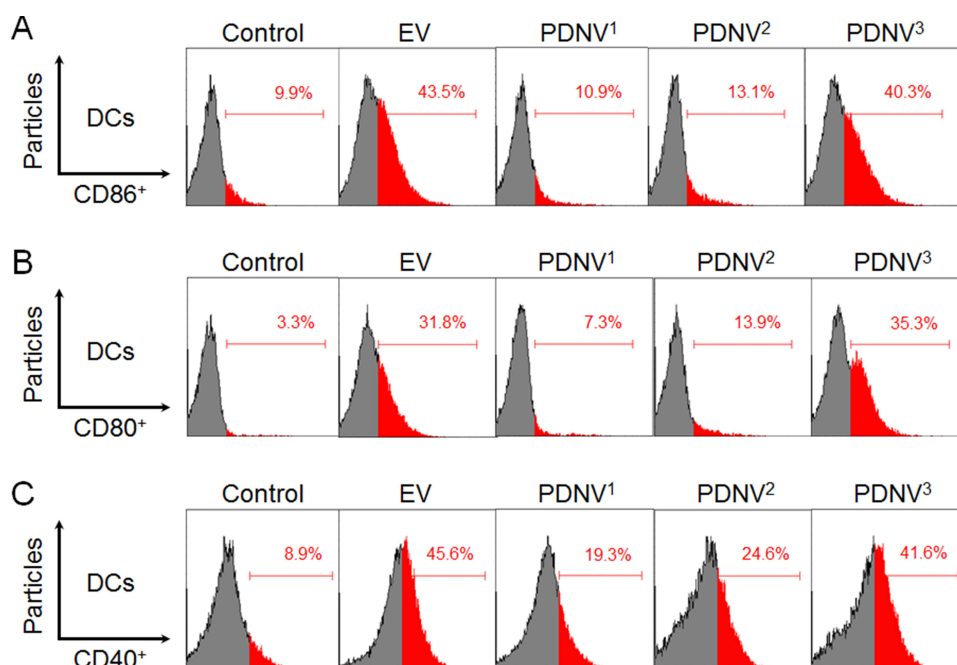


**Figure 4** DC cellular maturation induced by PDNVs with different sizes in the draining lymph nodes in vivo. Expression of CD86 (A), CD80 (B), and CD40 (C) on CD11c<sup>+</sup> DCs from inguinal lymph nodes of the mice was determined by flow cytometry (n = 6).

resident DCs to shuttle them to the lymph nodes. Moreover, several studies have reported smaller-sized nanoparticles are taken up more efficiently by DCs no matter in the injection site or lymph node. Therefore, the potent activation of DCs by PDNVs highlights the advantage of using small-sized vesicles for DC activation.

## Antibody Responses in Mice Triggered by PDNVs with Different Sizes

To investigate the ability of PDNV to induce bacterium-specific B cell responses, we next examined the antibody responses in mice. During the immunization process, the *S. aureus*-binding IgG titers were measured by collecting sera from mice of all groups.<sup>38,39</sup> As shown in Figure 5A, a continuous increase in *S. aureus*-binding IgG was detected in both PDNVs and EV groups, but not in PBS group during the period. The results showed that PDNV<sup>3</sup> induced higher bacterium-specific antibody titers compared with the PDNV<sup>1</sup> and PDNV<sup>2</sup>, which was similar with EV group. Beyond the titer levels, we also assessed the avidity against the source bacteria of sera collected from the immunized mice. As shown in Figure 5B, the significant enhancement of PDNV<sup>3</sup> in avidity index to the *S. aureus* bacteria compared with PDNV<sup>1</sup> and PDNV<sup>2</sup> was observed, which was comparable to the positive control. Dramatically, the avidity was increased with decreasing particle sizes. Overall, vaccination with PDNV<sup>3</sup> generated higher specific antibody responses and avidity to bacterium, indicating the potential of small-sized PDNVs for enhancing antibacterial immunity.

## T Cell Activated by PDNVs with Different Sizes in vivo

T cell-mediated immunity has become a crucial role in eliciting effective protection against bacterial infections.

The levels of IFN- $\gamma$  and IL-4 were used for quantifying T cell activation in the cell culture after restimulation of splenocytes by inactivated bacteria.<sup>40–42</sup> As shown in Figure 6A, the levels of IFN- $\gamma$  were higher in mice immunized with either PDNVs or EVs compared with the control mice, implying *S. aureus*-specific Th1 cell activation. The results also showed that mice immunized with PDNV<sup>3</sup> generated significantly higher levels of IFN- $\gamma$  ( $P < 0.05$ ) than PDNV<sup>1</sup> and PDNV<sup>2</sup> immunized mice, indicating a higher efficacy of small-sized PDNVs in activating T cells. However, the level of IL-4, a representative Th2 cytokine, showed no obvious changes in all the groups (Figure 6B). Altogether, the elevated production of IFN- $\gamma$  but not IL-4 suggested strong Th1 biased cell responses against the *S. aureus* bacteria infection.<sup>43–45</sup> On the contrary, Th2 biased cell response are usually associated with extracellular parasite infections or asthma, which was not activated by PDNVs immunization.

## Conclusion

In this study, we developed bacterial PDNVs with different sizes to study their ability as vaccine delivery system against drug-resistant *S. aureus* infection. Small-sized PDNVs showed better stability in biological buffer solutions than the large ones. In addition, our key findings demonstrate that as the vesicle size decreased, the DC maturation, B cell antibody response, and T cell response increased in PDNV immunized mice. PDNVs smaller than 200 nm induced significant improved B cell antibody response with high avidity than other sized PDNVs. In T cell-mediated immunity, the results showed PDNVs less than 200 nm elevated production of IFN- $\gamma$  significantly, indicating their ability to generate Th1 biased cell responses against the source bacteria. Overall,

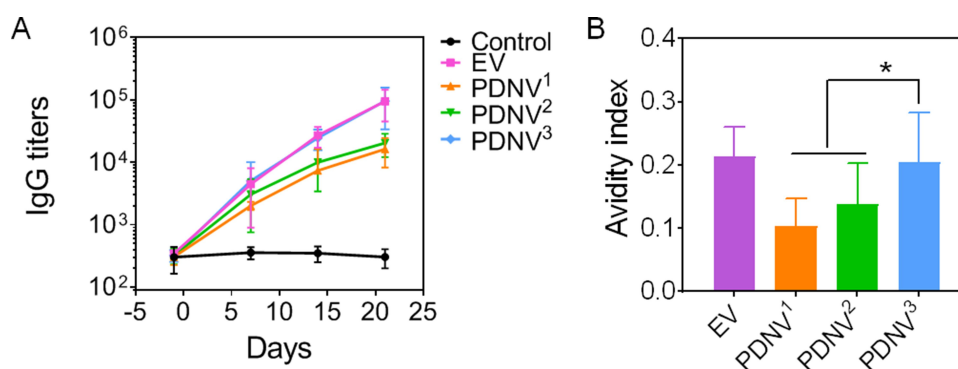


**Figure 5** Effects of PDNV size on antibody responses in vivo. (A) Time course of bacterium-specific IgG titers. (B) Quantified avidity index of the antisera from immunized mice binding to *S. aureus*. Data are presented as mean  $\pm$  SD ( $n = 6$ ). \* $P < 0.05$ , vs. indicated groups.

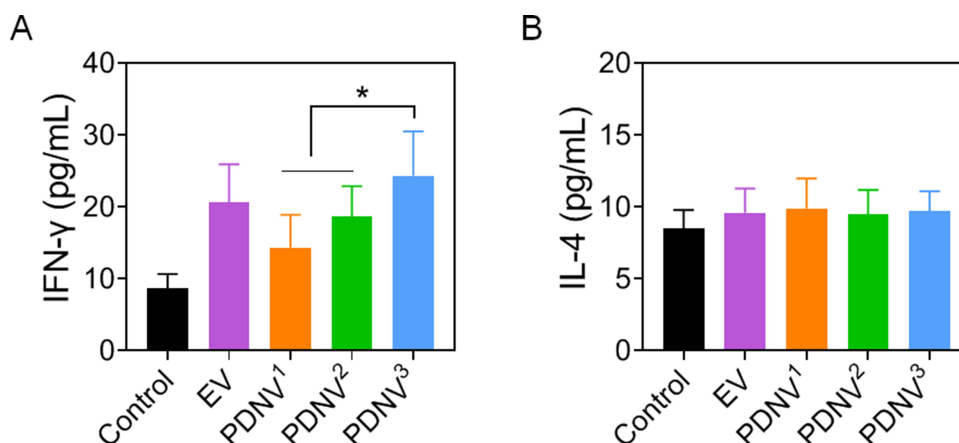


**Figure 6** Effects of PDNV size on bacterium-specific T cell activation in vivo. Amount of (A) IFN- $\gamma$  and (B) IL-4 in splenocyte supernatant after restimulation with *S. aureus*. Data are presented as the means  $\pm$  SD ( $n = 6$ ). \* $P < 0.05$ , vs. indicated groups.

PDNVs as promising multivalent antigen vaccines offer great potentials for designing effective antibacterial vaccines by size adjustment. The present study established the way towards the design of properly sized PDNVs with high vaccine efficacy. Our future studies will focus on comprehensive evaluation of the antigen presentation pathways, bio-distribution, vaccine efficacy in prophylactic and therapeutic models of PDNVs with different sizes.

## Abbreviations

*S. aureus*, *Staphylococcus aureus*; PDNVs, protoplast-derived nanovesicles; EVs, extracellular vesicles; APCs, antigen presenting cells; BMDCs, bone marrow-derived dendritic cells; DCs, dendritic cells; iDC, immature DC; mDC, mature DC; CTL, cytotoxic CD8<sup>+</sup> T lymphocytes; ELISA, enzyme-linked immunosorbent assay; IFN- $\gamma$ , interferon- $\gamma$ ; LB, Luria broth; LNs, lymph nodes; PBS, phosphate-buffered saline.

## Acknowledgments

This work was supported by the National Natural Science Foundation of China (Grant No: 31900993), the General and Special Financial Grant from the China Postdoctoral Science Foundation (Grant No: 2019M661956&2020T130561), the Postdoctoral Science Foundation Funded Project of Jiangsu Province (Grant No: 2019K066), the Engineering Research Center of Clinical Functional Materials and Diagnosis & Treatment Devices of Zhejiang Province (Grant No: WIBEK181007), the Start-up Fund provided by Yangzhou University (Grant No: 5020/137011461), the China CO-OP industry standardization project (2019GH-ZD-15), and the

Priority Academic Program Development of Jiangsu Higher Education Institutions (PAPD).

## Disclosure

The authors declared no conflicts of interest.

## References

1. Miller LS, Fowler VG, Shukla SK, Rose WE, Proctor RA. Development of a vaccine against *Staphylococcus aureus* invasive infections: evidence based on human immunity, genetics and bacterial evasion mechanisms. *FEMS Microbiol Rev*. 2020;44(1):123–153. doi:10.1093/femsre/fuz030
2. Lee AS, de Lencastre H, Garau J, et al. Methicillin-resistant *Staphylococcus aureus*. *Nat Rev Dis Primers*. 2018;4:18033. doi:10.1038/nrdp.2018.33
3. Makri A. Progress lags on vaccines to beat antimicrobial resistance. *Lancet*. 2019;394(10211):1793–1794. doi:10.1016/s0140-6736(19)32758-8
4. Tejal N, Gandhi MD, Malani PN. Combination Therapy for Methicillin-Resistant. *Staphylococcus Aureus Bacteremia*. 2020;0211. doi:10.15585/mmwr
5. Le P, Kunold E, Maccsics R, et al. Repurposing human kinase inhibitors to create an antibiotic active against drug-resistant *Staphylococcus aureus*, persisters and biofilms. *Nat Chem*. 2020;12(2):145–158. doi:10.1038/s41557-019-0378-76
6. Zhou Q, Wang T, Wang C, et al. Synthesis and characterization of silver nanoparticles-doped hydroxyapatite/alginate microparticles with promising cytocompatibility and antibacterial properties. *Colloid Surface A*. 2020;585:124081. doi:10.1016/j.colsurfa.2019.124081
7. Cordeiro AS, Alonso MJ. Recent advances in vaccine delivery. *Pharm Pat Anal*. 2016;5:49–73. doi:10.4155/ppa.15.38
8. Kong L, Zhang SM, Chu JH, et al. Tumor Microenvironmental Responsive Liposomes Simultaneously Encapsulating Biological and Chemotherapeutic Drugs for Enhancing Antitumor Efficacy of NSCLC. *Int J Nanomedicine*. 2020;15:6451–6468. doi:10.2147/IJN.S258906
9. Chi J, Ma Q, Shen Z, et al. Targeted nanocarriers based on iodinated-cyanine dyes as immunomodulators for synergistic phototherapy. *Nanoscale*. 2020;12(20):11008–11025. doi:10.1039/c9nr10674j
10. Brown L, Wolf JM, Prados-Rosales R, Casadevall A. Through the wall: extracellular vesicles in Gram-positive bacteria, mycobacteria and fungi. *Nat Rev Microbiol*. 2015;13(10):620–630. doi:10.1038/nrmicro3480



11. Kim OY, Dinh NTH, Park HT, Choi SJ, Hong K, Gho YS. Bacterial protoplast-derived nanovesicles for tumor targeted delivery of chemotherapeutics. *Biomaterials*. 2017;113:68–79. doi:10.1016/j.biomaterials.2016.10.037
12. Zhou J, Kroll AV, Holay M, Fang RH, Zhang L. Biomimetic Nanotechnology toward Personalized Vaccines. *Adv Mater*. 2020;32(13):e1901255. doi:10.1002/adma.201901255
13. Zhou X, Xie F, Wang L, et al. The function and clinical application of extracellular vesicles in innate immune regulation. *Cell Mol Immunol*. 2020;17(4):323–334. doi:10.1038/s41423-020-0391-1
14. Chen G, Bai Y, Li Z, Wang F, Fan X, Zhou X. Bacterial extracellular vesicle-coated multi-antigenic nanovaccines protect against drug-resistant *Staphylococcus* infection by modulating antigen processing and presentation pathways. *Theranostics*. 2020;10(16):7131–7149. doi:10.7150/thno.44564
15. Keller MD, Ching KL, Liang F-X, et al. Decoy exosomes provide protection against bacterial toxins. *Nature*. 2020;579(7798):260–264. doi:10.1038/s41586-020-2066-6
16. van der Pol L, Stork M, van der Ley P, van der Ley P. Outer membrane vesicles as platform vaccine technology. *Biotechnol J*. 2015;10(11):1689–1706. doi:10.1002/biot.201400395
17. Li M, Zhou H, Yang C, et al. Bacterial outer membrane vesicles as a platform for biomedical applications: an update. *J Controlled Release*. 2020;323:253–268. doi:10.1016/j.jconrel.2020.04.031
18. Mashburn-Warren L, McLean RJ, Whiteley M. Gram-negative outer membrane vesicles: beyond the cell surface. *Geobiology*. 2008;6(3):214–219. doi:10.1111/j.1472-4669.2008.00157.x
19. Kim OY, Choi SJ, Jang SC, et al. Bacterial protoplast-derived nanovesicles as vaccine delivery system against bacterial infection. *Nano Lett*. 2015;15(1):266–274. doi:10.1021/nl503508h
20. Benne N, van Duijn J, Kuiper J, Jiskoot W, Slutter B. Orchestrating immune responses: how size, shape and rigidity affect the immunogenicity of particulate vaccines. *J Control Release*. 2016;234:124–134. doi:10.1016/j.jconrel.2016.05.033
21. Hou C, Yi B, Jiang J, Chang Y-F, Yao X. Up-to-date vaccine delivery systems: robust immunity elicited by multifarious nanomaterials upon administration through diverse routes. *Biomaterials Sci*. 2019;7(3):822–835. doi:10.1039/C8BM01197D
22. Kumar S, Anselmo AC, Banerjee A, Zakrewsky M, Mitragotri S. Shape and size-dependent immune response to antigen-carrying nanoparticles. *J Control Release*. 2015;220(Pt A):141–148. doi:10.1016/j.jconrel.2015.09.069
23. Brewer JM, Pollock KGJ, Tetley L, Russell DG. Vesicle size influences the trafficking, processing, and presentation of antigens in lipid vesicles. *J Immunol*. 2004;173(10):6143–6150. doi:10.4049/jimmunol.173.10.6143
24. Krishnamurthy AT, Turley SJ. Lymph node stromal cells: cartographers of the immune system. *Nat Immunol*. 2020;21(4):369–380. doi:10.1038/s41590-020-0635-3
25. de Jong SE, Olin A, Pulendran B. The Impact of the Microbiome on Immunity to Vaccination in Humans. *Cell Host Microbe*. 2020;28(2):169–179. doi:10.1016/j.chom.2020.06.014
26. Rasmus Iversen R, Sollid LM. Autoimmunity provoked by foreign antigens. *Science*. 2020;368(6487):132–133. doi:10.1126/science.aay3037
27. Kang S, Ahn S, Lee J, et al. Effects of gold nanoparticle-based vaccine size on lymph node delivery and cytotoxic T-lymphocyte responses. *J Control Release*. 2017;256:56–67. doi:10.1016/j.jconrel.2017.04.024
28. Chen X, Gao C. Influences of size and surface coating of gold nanoparticles on inflammatory activation of macrophages. *Colloids Surf B Biointerfaces*. 2017;160:372–380. doi:10.1016/j.colsurfb.2017.09.046
29. Huang X, Li L, Liu T, et al. The Shape Effect of Mesoporous Silica Nanoparticles on Biodistribution, Clearance, and Biocompatibility in Vivo. *ACS Nano*. 2011;5(7):5390–5399. doi:10.1021/nn200365a
30. Manolova V, Flace A, Bauer M, Schwarz K, Saudan P, Bachmann M. Nanoparticles target distinct dendritic cell populations according to their size. *Eur J Immunol*. 2008;38(5):1404–1413. doi:10.1002/eji.200737984
31. Chang TZ, Stadtmiller SS, Staskevicius E, Champion JA. Effects of ovalbumin protein nanoparticle vaccine size and coating on dendritic cell processing. *Biomater Sci*. 2017;5(2):223–233. doi:10.1039/c6bm00500d
32. Schooling SR, Beveridge TJ. Membrane vesicles: an overlooked component of the matrices of biofilms. *J Bacteriol*. 2006;188(16):5945–5957. doi:10.1128/JB.00257-06
33. Gao W, Fang RH, Thamphiwatana S, et al. Modulating antibacterial immunity via bacterial membrane-coated nanoparticles. *Nano Lett*. 2015;15(2):1403–1409. doi:10.1021/nl504798g
34. Wu Q, Gen W, Zhuobin X, et al. Mechanistic Insight into the Light-Irradiated Carbon Capsules as an Antibacterial Agent. *ACS Appl Mater Interfaces*. 2014;8b04932.
35. Srinivas R, Garu A, Moku G, Agawane SB, Chaudhuri A. A long-lasting dendritic cell DNA vaccination system using lysinylated amphiphiles with mannose-mimicking head-groups. *Biomaterials*. 2012;33(26):6220–6229. doi:10.1016/j.biomaterials.2012.05.006
36. Yoshizaki Y, Yuba E, Sakaguchi N, Koiwai K, Harada A, Kono K. pH-sensitive polymer-modified liposome-based immunity-inducing system: effects of inclusion of cationic lipid and CpG-DNA. *Biomaterials*. 2017;141:272–283. doi:10.1016/j.biomaterials.2017.07.001
37. Yang W, Zhu G, Wang S, et al. In Situ Dendritic Cell Vaccine for Effective Cancer Immunotherapy. *ACS Nano*. 2019;13(3):3083–3094. doi:10.1021/acsnano.8b08346
38. Chen G, Wang Y, Wu P, et al. Reversibly Stabilized Polycation Nanoparticles for Combination Treatment of Early- and Late-Stage Metastatic Breast Cancer. *ACS Nano*. 2018;12(7):6620–6636. doi:10.1021/acsnano.8b01482
39. Pang X, Liu X, Cheng Y, et al. Sono-Immunotherapeutic Nanocapturer to Combat Multidrug-Resistant Bacterial Infections. *Adv Mater*. 2019;31(35):e1902530. doi:10.1002/adma.201902530
40. Rao L, Tian R, Cell-Membrane-Mimicking CX. Nanodecoys against Infectious Diseases. *ACS Nano*. 2020;14(3):2569–2574. doi:10.1021/acsnano.0c01665
41. Ying M, Zhuang J, Wei X, et al. Remote-Loaded Platelet Vesicles for Disease-Targeted Delivery of Therapeutics. *Adv Funct Mater*. 2018;28:22. doi:10.1002/adfm.201801032
42. Hui J, Dong PT, Liang L, et al. Photo-Disassembly of Membrane Microdomains Revives Conventional Antibiotics against MRSA. *Adv Sci*. 2020;7(6):1903117. doi:10.1002/advs.201903117
43. Wang F, Fang RH, Luk BT, et al. Nanoparticle-Based Antivirulence Vaccine for the Management of Methicillin-Resistant *Staphylococcus aureus* Skin Infection. *Adv Funct Mater*. 2016;26(10):1628–1635. doi:10.1002/adfm.201505231
44. Wu Y, Song Z, Wang H, Han H. Endogenous stimulus-powered antibiotic release from nanoreactors for a combination therapy of bacterial infections. *Nat Commun*. 2019;10:1. doi:10.1038/s41467-019-12233-2
45. Tang S, Zhang F, Gong H, et al. Enzyme-powered Janus platelet cell robots for active and targeted drug delivery. *Sci Robotics*. 2020;5:43. doi:10.1126/scirobotics.aba6137

**International Journal of Nanomedicine****Dovepress****Publish your work in this journal**

The International Journal of Nanomedicine is an international, peer-reviewed journal focusing on the application of nanotechnology in diagnostics, therapeutics, and drug delivery systems throughout the biomedical field. This journal is indexed on PubMed Central, MedLine, CAS, SciSearch®, Current Contents®/Clinical Medicine,

Journal Citation Reports/Science Edition, EMBase, Scopus and the Elsevier Bibliographic databases. The manuscript management system is completely online and includes a very quick and fair peer-review system, which is all easy to use. Visit <http://www.dovepress.com/testimonials.php> to read real quotes from published authors.

Submit your manuscript here: <https://www.dovepress.com/international-journal-of-nanomedicine-journal>